



Contents lists available at ScienceDirect

Mechatronics

journal homepage: www.elsevier.com/locate/mechatronics

Subspace predictive repetitive control to mitigate periodic loads on large scale wind turbines

S.T. Navalkar^{a,*}, J.W. van Wingerden^a, E. van Solingen^a, T. Oomen^b, E. Pasterkamp^c, G.A.M. van Kuik^d

^a Delft Center for Systems and Control, Faculty of Mechanical Engineering, Delft University of Technology, 2628 CD Delft, The Netherlands

^b Control Systems Technology Group, Department of Mechanical Engineering, Eindhoven University of Technology, 5600 MB Eindhoven, The Netherlands

^c XEMC Darwind BV, Oude Enghweg 2, 1217 JC Hilversum, The Netherlands

^d Wind Energy Group, Faculty of Aerospace Engineering, Delft University of Technology, Kluyverweg 1, 2629 HS Delft, The Netherlands

ARTICLE INFO

Article history:

Received 26 September 2013

Revised 23 December 2013

Accepted 6 January 2014

Available online xxx

Keywords:

Subspace predictive control

Repetitive control

System identification

Wind turbine vibration control

IPC

ABSTRACT

Manufacturing and maintenance costs arising out of wind turbine dynamic loading are one of the largest bottlenecks in the roll-out of wind energy. Individual Pitch Control (IPC) is being researched for cost reduction through load alleviation; it poses a challenging mechatronic problem due to its multi-input, multi-output (MIMO) nature and actuation constraints related to the wear of pitch bearings. To address these issues, Subspace Predictive Repetitive Control (SPRC), a novel repetitive control strategy based on the subspace identification paradigm, is presented. First, the Markov parameters of the system are identified online in a recursive manner. These parameters are used to build up the lifted matrices needed to predict the output over the next period. From these matrices an adaptive repetitive control law is derived. To account for actuator limitations, the known shape of wind-induced disturbances is exploited to perform repetitive control in a reduced-dimension basis function subspace. The SPRC methodology is implemented on a high-fidelity numerical aeroelastic environment for wind turbines. Load reductions are achieved similar to those obtained with classical IPC approaches, while considerably limiting the frequency content of the actuator signals.

© 2014 Elsevier Ltd. All rights reserved.

1. Introduction

In the past three decades, wind energy has shown exponential growth, reaching an installed capacity of 282 GW in 2012, capable of delivering 3% of the global electricity demand. As a clean, resource-efficient source of energy, wind power is viewed as a viable complement to the current energy mix, with more than a 100 countries actively investing in large-scale wind energy [1]. A majority of commercial wind turbines are multi-megawatt grid-connected machines, installed onshore. It is expected that offshore siting of wind farms will gain further momentum in the future, as this affords the opportunity to tap higher wind speeds and relaxes the constraints imposed by sites close to densely populated areas. However, one of the main roadblocks to offshore wind energy development is the high capital cost associated with the design of a mechanical system able to withstand severe dynamic loading, of the order of 10^8 to 10^9 loading cycles, significantly higher than any other commercially produced mechanical component [2].

Further, the relative inaccessibility of the offshore environment exacerbates repair and maintenance issues.

Turbines are today instrumented with a variety of sensors and new actuators; thus mechatronics and control engineering form an integral part of wind turbine design. The highly coupled aerodynamic-structural interactions and the electromechanical conversion to grid-quality electrical energy requires sophisticated control strategies and the use of the latest advances in sensor and power electronics. One of the first comprehensive analyses of this mechatronic and control problem [3], highlights the need for optimal multivariable control design of modern wind turbines for load reduction and controller validation on high-fidelity simulators.

For load control, individual pitch control (IPC) is perhaps one of the most interesting and readily implementable extensions to the basic controller [4]. In recent literature, PI (proportional-integral) control has been used for implementing IPC on prototypes. However, since the system is periodic and multi-input, multi-output (MIMO) in nature, it is difficult to achieve the precise control within narrow frequency bands typically seen in wind turbine loads. Although important improvements have been made, at present the control techniques do not exploit the periodic nature of the disturbances. Hence, current control techniques cannot achieve the

* Corresponding author. Tel.: +31 623721917.

E-mail addresses: S.T.Navalkar@tudelft.nl (S.T. Navalkar), J.W.vanWingerden@tudelft.nl (J.W. van Wingerden), E.vanSolingen@tudelft.nl (E. van Solingen), T.A.E.Oomen@tue.nl (T. Oomen), E.Pasterkamp@xemc-darwind.com (E. Pasterkamp), G.A.M.vanKuik@tudelft.nl (G.A.M. van Kuik).

limits of performance, and require a significant amount of control effort across a broad spectrum of frequencies.

In control engineering literature, several high-performance approaches have been developed to specifically target periodic disturbances. Learning control, of the form first introduced in [5], achieves asymptotic rejection of periodic disturbances by “learning”, in real-time, the ideal feedforward control input sequence thereto. The term “Iterative Learning Control (ILC)” is used to designate those learning control problems where the initial conditions are reset at the end of each period, while “Repetitive Control (RC)” is used to designate those problems where the final conditions of the previous period are the initial conditions of the current period. Since a wind turbine does not undergo initial condition resets, load reduction forms an RC problem, but the two methodologies are very closely related. The survey paper [6] reviews the different approaches towards designing ILC controllers, and delineates conditions for satisfying the stability, performance and robustness criteria. ILC control has been shown to achieve performance superior to that of a traditional 2-DoF controller in tracking applications [7]. The use of ILC for vibration rejection of flexible structures using Hankel matrices has been shown in [8], with excellent potential for online adaptive control. The receding horizon principle of Model Predictive Control (MPC) has been combined with RC in [9] to obtain a predictive-repetitive controller capable of handling constraints. It should be noted, however, that all the RC methods mentioned above are model-based and cannot be directly applied to an unknown plant.

For the current application, model-based RC has been simulated in [10], specifically to target all periodic loads with a single control loop. It can easily deal with the MIMO problem with a transparent LQR formulation. RC design involves recursively optimising the lifted control input; for many systems this has a very high dimensionality. To robustify the performance of the RC, the dimensionality can be reduced by projecting the control input onto a basis function subspace, chosen such that the basis vector directions capture a large amount of energy content of the periodic disturbance [11,12]. In [13], load reduction was achieved by using RC with sinusoidal basis functions, on a scaled prototype wind turbine in a real-time wind tunnel experiment. Here, instead of using pitch actuation, active flaps located on the blades were used to control the aerodynamic flow and thereby achieve load reduction. As the number of actuators available for control increases, state-of-the-art decoupled PI controllers can no longer provide optimal control inputs, and a true MIMO strategy, like RC, seems to be necessary. However, in all the above cases, the RC control law was derived based on the assumption that the plant model is available and is perfectly LTI.

Although RC controllers can be substantially robust to model uncertainties, it may prove difficult in practical cases to arrive at an approximate system model of a wind turbine. Aerodynamic control authority is a strong function of mean free stream wind speed, a slowly varying environmental parameter, which currently cannot be reliably measured or estimated in wind turbines. Wind turbine dynamics also depend on turbine location and manufacturing discrepancies (e.g. rotor imbalance), and are hence unique to each turbine. So, an adaptive control strategy which is able to identify wind turbine dynamics online, would be most suitable for IPC.

Different adaptive methods have been explored for combining learning control with online identification. In [14], the concept of basis functions optimised for the unknown system directly from input–output data is introduced. In [15], offline system identification is done in the basis function domain and applied to a robotic arm for ILC position control. However, there has thus far not been a formalised combination of online system identification and learning control that would be amenable to further analysis as a fully adaptive control law.

Subspace identification, described in [16] can be readily adapted for online system identification of engineering systems in both open- and closed-loop settings. As introduced in [17], subspace identification can be integrated with receding horizon predictive control to achieve model-less online adaptive control; this control technique is called Subspace Predictive Control (SPC). This has been applied to aeroelastic vibration control of wind turbines in [18], and appears to be directly extendable to incorporate RC for suppressing periodic disturbances.

The key contribution of this paper is a novel RC approach that utilises online system identification to form an adaptive control law for periodic disturbances, the so-called “Subspace Predictive Repetitive Controller” (SPRC). This controller is formulated to asymptotically suppress the dominant periodic loads in the turbine, as per RC theory. Further, basis functions are used to enable tight control over the shape of the actuator signals, a significant advantage for limiting actuator stress. The integration with online system identification ensures that controller performance can be maximised irrespective of variations or variability in the dynamics of the wind turbine system. The validity of this approach is proved by application to the highly complex wind turbine mechatronic system, tested in a high fidelity numerical environment. As a predictive-repetitive scheme, SPRC can be directly extended to include constraints, however this has not been explored in the current paper.

The outline of the paper is as follows: in Section 2 the background for IPC is explained and the simulation environment is described. In Section 3 the methodology of SPRC is introduced. In Section 4, the results are presented, and conclusions drawn from these results will be discussed in Section 5.

2. Control of wind turbines

A modern wind turbine is a large-scale mechatronic system, with a complex interplay between actuating and power transfer mechanisms, the electrical drives and the control electronics. The main components relevant from the perspective of dynamic load alleviation are described below [19]:

- *Rotor* – The rotor consists of a hub supporting up to three blades, free to rotate on a horizontal axis. Aerodynamic torque is generated by wind flowing through the rotor disc.
- *Transmission* – The rotation of the rotor is transmitted by the main shaft, supported on the main bearings, to the generator located in the housing (nacelle) of the turbine. A gearbox may be used to change the speed of rotation if required.
- *Generator* – The generator converts the rotation of the output shaft into electrical energy. The generated electricity is then conditioned by a converter and a transformer to make it suitable for grid upload.
- *Support Structure* – This includes the tower and all other structural elements required to support the nacelle and the rotor, and withstand the loading over the lifetime of the wind turbine, typically taken to be 20 years.

These components can be seen in Fig. 1, which shows the prototype turbine XEMC-Darwind XD115 in full and cross-sectional views. This testing prototype has been constructed at Wieringerwerf in the Netherlands. A high-fidelity model of this turbine will be considered as our test bench in the rest of the paper.

The operation of a wind turbine is divided into two regions: the region where the wind speed is below the rated wind speed of the turbine, and the region where it is above the rated wind speed. In the below-rated region, the wind turbine is expected to maximise the energy that can be extracted from the air stream. In the

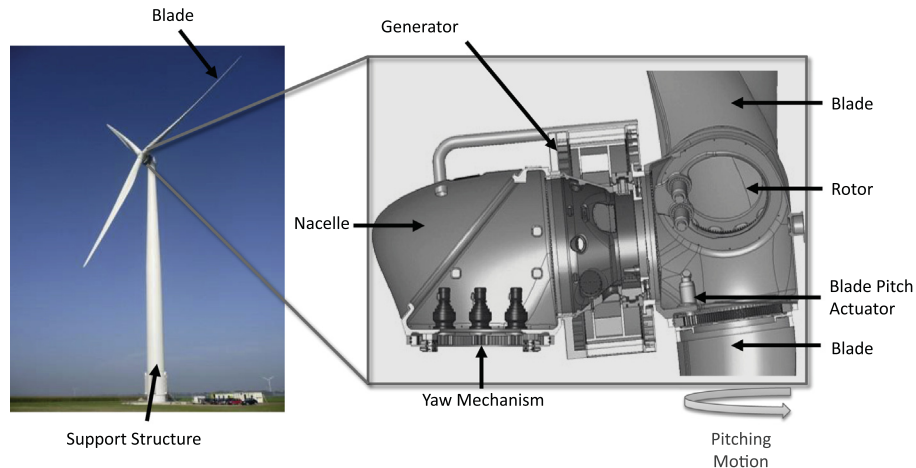


Fig. 1. XEMC-Darwind XD115 wind turbine: full and cross-sectional views [20].

above-rated region, the wind turbine has to produce the power dictated by the rated power of the generator, and avoid overspeeding for safe operation. Thus, both the conventional wind turbine control objectives are related to energy capture. Today, wind turbines are also implemented with the control objective of minimisation of dynamic loads, which are the structural design drivers for blades and the support structure: their reduction directly translates to material and thus cost reduction.

As portrayed in Fig. 2, wind turbine control can be divided into (a) baseline control, which encompasses all the blocks enclosed within the solid line, and (b) new load control strategies, which can be appended, in closed-loop with the baseline controlled system, as exemplified by the SPRC controller outside the dotted line.

2.1. Baseline control

The objective of power production control requires that maximum energy is captured in the below-rated region, while power is regulated to rated power in the above-rated region. Both these objectives can be achieved by regulating the generator speed to follow a reference trajectory. In the below-rated region, the generator torque is used as a control input, and modified such that it bears a constant ratio to the square of generator speed, which

ensures maximum power capture [19]. The torque command is also manipulated to avoid excessive dwell-time at those generator speeds that coincide with structural frequencies.

In the above-rated region, generator torque is kept constant. Aerodynamic torque is manipulated to regulate the generator speed to its rated value. All three blades are collectively pitched along their axes, using gain-scheduled PI control. Basic SISO (single-input single-output) controllers, designed independently of the other controllers, are also used to add damping to structural resonances, typically the drive train torsional mode and the fore-aft tower bending mode, using generator torque or collective pitch as the control input. Feedback for these controllers is obtained from direct measurement using accelerometers or via state estimation.

In [21] the complete control design for a typical commercial wind turbine is presented. This controller is capable of tracking the desired power-wind speed characteristics. It also encompasses basic load reduction at structural modes. Such a controller may be considered to be the state of the art for most turbines in the field today [22], and is deemed the baseline controller in the context of this paper. However, the dominant dynamic loading in a wind turbine occurs at the rotational frequency of the turbine rotor (1P) and its harmonics (2P, 3P, ...) is not addressed by this controller. This loading is asymmetric and as such cannot be attenuated

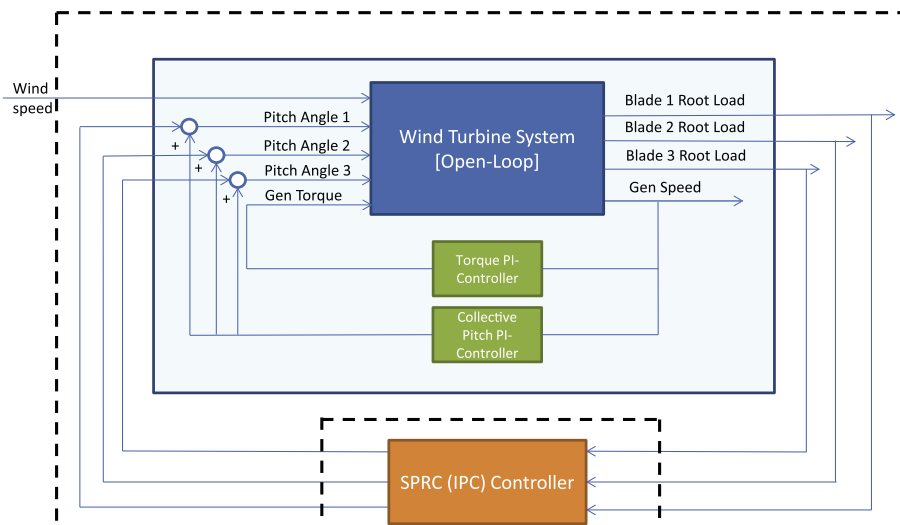


Fig. 2. Wind turbine control block diagram.

using torque or collective pitch control, which motivates the concept of Individual Pitch Control (IPC) for load reduction.

2.2. Individual pitch control

To facilitate collective pitch control, wind turbines today are equipped with hydraulic or electrical pitch actuators which can rotate (or *pitch*) each blade individually along its longitudinal axis. Taking a parallel from the helicopter industry, it was postulated that load reduction could be achieved by pitching the blades independently, a methodology known as Individual Pitch Control (IPC). IPC explicitly targets blade loading at 1P, 2P, . . . [4], which form the dominant component of the dynamic loading.

The feedback for IPC is usually obtained from strain gauges located at the base of each blade. For a commercial three-bladed wind turbine, this results in a MIMO, or more specifically, a rotating 3×3 system that needs to be controlled. The controller used in most of the prototype implementations is the multi-blade co-ordinate (MBC)-based controller, as described by [23–26], obtained by decoupling the MIMO wind turbine system via the MBC transform and using one PI controller per loop. Using the transformation, the system is converted to an LTI system, and a simple PI control design can be effectuated to implement IPC.

This approach does not exploit the special structure of the disturbance, and its performance can be potentially improved by RC. This MBC controller will be further used in the results section to facilitate comparison with the SPRC controller.

2.3. Testing environment

Control design validation has been carried out using the software GH Bladed 4.0TM from Garrad Hassan & Partners Ltd. This certified wind turbine design software has been benchmarked against wind turbine experimental data and used in recent literature to compare wind turbine load reduction strategies [27]. GH BladedTM provides a high-fidelity numerical prototyping environment that forms an industry-accepted test bench for the purpose of evaluating new control strategies, advanced aerodynamic blade design capabilities and the ability to incorporate different advanced actuator designs. It has the following characteristics:

- The widely-accepted blade element momentum theory is used with wake and dynamic stall corrections to define aeroelastic interactions.
- A multi-body dynamics approach is used to model the structural response of the wind turbine. The blades and the tower are taken to be flexible bodies, with a user-defined number of flexible modes.
- Realistic wind fields can be generated, with turbulence, wind shear and gusts.
- Although built-in PI controllers can be used for baseline control, it is also possible to interface a user-defined dll. In the current case, a Matlab-Simulink environment is used to compile a controller dll with the learning control strategy, in order to evaluate its suitability for the application.

The Bladed model of the XEMC-Darwind XD115 5 MW machine, a commercial wind turbine currently in the development phase, is used for testing purposes. Its general characteristics are given in the Table 1. A nominal controller connected with this model, which covers the baseline control objectives stated above, is used as reference controller. The new repetitive controller designed within this paper is then connected in feedback with the baseline closed-loop system, to evaluate the load reduction potential.

Table 1
XEMC-Darwind XD115 Wind Turbine specifications [20].

Description	Symbol	Value
Rated power	P_{rated}	5000 kW
Rotor diameter	d_{ro}	115 m
Cut-in wind speed	v_{cutin}	4 m/s
Rated wind speed	v_{rated}	12 m/s
Cut-out wind speed	v_{cutout}	25 m/s
Rated rotational rotor speed	Ω_{ro}	18 rpm
Gearbox ratio	γ	1.0 (Direct-Drive)
Pitch-rate limit	$\dot{\theta}_{\text{limit}}$	6°/s

3. SPRC control methodology

In this section the assumptions made and the steps taken in implementing an SPRC control law for the purpose of IPC are delineated. First, the system is defined and an output predictor is formulated which will be used in deriving the control law. Then, the required system parameters are identified online. Finally, these parameters are manipulated to obtain a repetitive control law which minimises the vibration output over an infinite horizon.

3.1. Step 1: System definition and predictor formulation

A wind turbine can be approximated by a discrete-time LTI (linear, time-invariant) system with unknown periodic disturbances [10]:

$$x_{k+1} = Ax_k + Bu_k + Ed_k + Ke_k, \quad (1)$$

$$y_k = Cx_k + Du_k + Fd_k + e_k, \quad (2)$$

where $x_k \in \mathbb{R}^n$ is the state vector. $u_k \in \mathbb{R}^r$ is the control input vector; for the case of IPC this consists of the three blade pitch angles, thus, $r = 3$. The output vector $y_k \in \mathbb{R}^l$ is fed back to the controller, which consists of turbine loads (e.g. blade root bending moments), measured by strain gauges or equivalent sensors. An artificial periodic disturbance vector $d_k \in \mathbb{R}^m$ represents the periodic component of the loading at the blade root, while $e_k \in \mathbb{R}^l$ denotes the zero mean white innovation process, or physically, the aperiodic component of the blade root loading. The matrices ($A \in \mathbb{R}^{n \times n}$, $B \in \mathbb{R}^{n \times r}$, $C \in \mathbb{R}^{l \times n}$, $D \in \mathbb{R}^{l \times r}$, $K \in \mathbb{R}^{n \times l}$, $E \in \mathbb{R}^{n \times m}$, $F \in \mathbb{R}^{l \times m}$) are the state transition, input, output, direct feedthrough, observer, periodic noise input and periodic noise direct feed through matrices, respectively. Substituting (2) in (1):

$$x_{k+1} = \tilde{A}x_k + \tilde{B}u_k + \tilde{E}d_k + Ky_k, \quad (3)$$

$$y_k = Cx_k + Du_k + Fd_k + e_k, \quad (4)$$

with

$$\tilde{A} = A - KC, \quad \tilde{B} = B - KD, \quad \tilde{E} = E - KF.$$

Since d_k is an unknown but periodic disturbance, its effect on the input–output behaviour of the plant is eliminated by defining a periodic difference operator δ :

$$\delta y_k = y_k - y_{k-P},$$

$$\delta u_k = u_k - u_{k-P},$$

$$\delta d_k = d_k - d_{k-P} = 0,$$

where P is the period of the periodic disturbance. Applying the δ operator to the system (3) and (4), we get the differenced system:

$$\delta x_{k+1} = \tilde{A}\delta x_k + \tilde{B}\delta u_k + K\delta y_k, \quad (5)$$

$$\delta y_k = C\delta x_k + D\delta u_k + \delta e_k. \quad (6)$$

For deriving a repetitive control law, it is essential to formulate the output over the next period as a function of the control input.

Based on this, the control input can be optimised to minimise the vibration output and achieve disturbance rejection. Hence, the first step is to obtain a predictor assuming that the system dynamics are known. The differenced state δx_{k+p} is expressed in terms of input–output data:

$$\delta x_{k+p} = \tilde{A}^p \delta x_k + \begin{bmatrix} \mathcal{H}_u^{(p)} & \mathcal{H}_y^{(p)} \end{bmatrix} \begin{bmatrix} \delta U_k^{(p)} \\ \delta Y_k^{(p)} \end{bmatrix}. \quad (7)$$

where the stacked vectors are defined as:

$$\delta U_k^{(s)} = \begin{bmatrix} u_k - u_{k-p} \\ u_{k+1} - u_{k+1-p} \\ \vdots \\ u_{k+s-1} - u_{k+s-1-p} \end{bmatrix},$$

and a similar vector $Y_k^{(s)}$ for the signal y_k . The extended controllability matrix is defined as:

$$\mathcal{H}^{(p)} = \begin{bmatrix} \mathcal{H}_u^{(p)} & \mathcal{H}_y^{(p)} \end{bmatrix},$$

with:

$$\begin{aligned} \mathcal{H}_u^{(p)} &= \begin{bmatrix} \tilde{A}^{p-1} \tilde{B} & \tilde{A}^{p-2} \tilde{B} & \dots & \tilde{B} \end{bmatrix}, \\ \mathcal{H}_y^{(p)} &= \begin{bmatrix} \tilde{A}^{p-1} K & \tilde{A}^{p-2} K & \dots & K \end{bmatrix}, \end{aligned}$$

where p is the past window. The key approximation in this algorithm is that we assume that $\tilde{A}^j \approx 0$ for all $j \geq p$. It can be shown that if the system in (3) and (4) is stable, the approximation error can be made arbitrarily small by making p sufficiently large [28]. Note that even if the system is not stable, but satisfies stability requirements, an observer gain K can always be defined such that the system (3) and (4) is stable. With this assumption the differenced state δx_{k+p} is approximately given by:

$$\delta x_{k+p} \approx \begin{bmatrix} \mathcal{H}_u^{(p)} & \mathcal{H}_y^{(p)} \end{bmatrix} \begin{bmatrix} \delta U_k^{(p)} \\ \delta Y_k^{(p)} \end{bmatrix}.$$

For repetitive control, it is necessary to predict the output over one entire period P , where $P \geq p$, but is usually much larger. Lifting the output equation over the period P :

$$\delta Y_{k+p}^{(P)} = \tilde{I}^{(P)} \delta x_k + \begin{bmatrix} \tilde{H}^{(P)} & \tilde{G}^{(P)} \end{bmatrix} \begin{bmatrix} \delta U_{k+p}^{(P)} \\ \delta Y_{k+p}^{(P)} \end{bmatrix}. \quad (8)$$

As this is a predictor, the white noise sequence δe_k is omitted,

$$\delta Y_{k+p}^{(P)} \approx \begin{bmatrix} \tilde{I}^{(P)} \mathcal{H}_u^{(p)} & \tilde{I}^{(P)} \mathcal{H}_y^{(p)} \end{bmatrix} \begin{bmatrix} \delta U_k^{(p)} \\ \delta Y_k^{(p)} \end{bmatrix} + \begin{bmatrix} \tilde{H}^{(P)} & \tilde{G}^{(P)} \end{bmatrix} \begin{bmatrix} \delta U_{k+p}^{(P)} \\ \delta Y_{k+p}^{(P)} \end{bmatrix}. \quad (9)$$

Here, the Toeplitz matrix $\tilde{H}^{(P)}$ is defined as:

$$\tilde{H}^{(P)} = \begin{bmatrix} D & 0 & 0 & \dots & 0 \\ \tilde{C}\tilde{B} & D & 0 & \dots & 0 \\ \tilde{C}\tilde{A}\tilde{B} & \tilde{C}\tilde{B} & D & \dots & 0 \\ \vdots & \vdots & \vdots & \ddots & \vdots \\ \tilde{C}\tilde{A}^{p-1}\tilde{B} & \tilde{C}\tilde{A}^{p-2}\tilde{B} & \tilde{C}\tilde{A}^{p-3}\tilde{B} & \dots & 0 \\ 0 & \tilde{C}\tilde{A}^{p-1}\tilde{B} & \tilde{C}\tilde{A}^{p-2}\tilde{B} & \dots & 0 \\ 0 & 0 & \tilde{C}\tilde{A}^{p-1}\tilde{B} & \dots & 0 \\ \vdots & \vdots & \vdots & \ddots & \vdots \\ 0 & 0 & 0 & \dots & D \end{bmatrix}. \quad (10)$$

In a similar way, replacing \tilde{A} by A and \tilde{B} by B , the matrix $H^{(P)}$ can be defined. A similar substitution can be done to obtain $\tilde{G}^{(P)}$ and

$G^{(P)}$ by replacing \tilde{B} and B both by K . Finally, the extended observability matrix, $\tilde{I}^{(P)}$ is defined as:

$$\tilde{I}^{(P)} = \begin{bmatrix} C \\ \tilde{C}\tilde{A} \\ \vdots \\ \tilde{C}\tilde{A}^{p-1} \\ 0 \\ 0 \\ \vdots \\ 0 \end{bmatrix}. \quad (11)$$

The matrix $\Gamma^{(P)}$ can be defined by replacing \tilde{A} by A . Now the extended observability times controllability matrix in the Eq. (9) is given by:

$$\tilde{I}^{(P)} \mathcal{H}_u^{(p)} \approx \begin{bmatrix} \tilde{C}\tilde{A}^{p-1}\tilde{B} & \tilde{C}\tilde{A}^{p-2}\tilde{B} & \dots & \tilde{C}\tilde{B} \\ 0 & \tilde{C}\tilde{A}^{p-1}\tilde{B} & \dots & \tilde{C}\tilde{A}\tilde{B} \\ \vdots & & \ddots & \\ 0 & & & \tilde{C}\tilde{A}^{p-1}\tilde{B} \end{bmatrix}.$$

A similar expression can be generated for $\tilde{I}^{(P)} \mathcal{H}_y^{(p)}$. The objective of the identification is to estimate these matrices, as well as the Toeplitz matrices described above. Considering the first block row of Equation (9), we have:

$$\delta y_{k+p} = \begin{bmatrix} C \mathcal{H}_u^{(p)} & C \mathcal{H}_y^{(p)} \end{bmatrix} \begin{bmatrix} \delta U_k^{(p)} \\ \delta Y_k^{(p)} \end{bmatrix}. \quad (12)$$

It can be seen that the matrix of coefficients $\begin{bmatrix} C \mathcal{H}_u^{(p)} & C \mathcal{H}_y^{(p)} \end{bmatrix}$ contains all the information required to construct the $\tilde{I}^{(P)} \mathcal{H}^{(p)}$ and the Toeplitz matrices required above. Hence, the aim of the identification is to solve the regression problem constituted by the Eq. (12) recursively in an online manner, as and when input–output data becomes available.

3.2. Step 2: Identification

The identification problem can now be formulated as: given the input sequence u_k and the output sequence y_k available over the time horizon $[k - P, \dots, k]$; estimate recursively the set of parameters Ξ that uniquely define the dynamics of the system (1) and (2). It is postulated here that these are the Markov parameters of the differenced system in the predictor form:

$$\Xi = \begin{bmatrix} C \mathcal{H}_u^{(p)} & C \mathcal{H}_y^{(p)} \end{bmatrix}. \quad (13)$$

This identification problem has the following features:

- Although many wind turbines are (critically) stable in the open loop, for safety reasons they are almost never operated in production mode without a controller in the loop. Thus, it is necessary to do closed-loop system identification.
- The feedback controller used with the wind turbine system during identification should be close to the optimal controller that will later be devised; this ensures that deviations from the operating point are minimised, and plant behaviour can be approximated better by a linear model.
- Since identification is to be done online, a recursive system identification strategy would be appropriate. Such a strategy is required to be both stable and show rapid convergence.

The predicted output at any time instant can be stated purely in terms of past input–output data, as in Eq. (12). This implies that

the Markov parameters can be found within the subspace defined by the past input–output data.

The regression problem is stated mathematically below. If the differenced output is given by

$$\delta y_k = \Xi \begin{bmatrix} \delta U_k^{(p)} \\ \delta Y_k^{(p)} \end{bmatrix} + \delta e_k, \quad (14)$$

uniquely compute the matrix Ξ , in a recursive manner, at every time instant k , as the solution to:

$$\Xi = \arg \min_{\Xi} \sum_{k=0}^{\infty} \left\| \delta y_k - \Xi \begin{bmatrix} \delta U_k^{(p)} \\ \delta Y_k^{(p)} \end{bmatrix} \right\|_2^2. \quad (15)$$

To obtain a unique solution to this least squares problem, it is of key importance that the matrix $[(\delta U_k^{(p)})^T, (\delta Y_k^{(p)})^T]^T$ has full rank at all time steps k . The rank of this matrix is dependent on the input signal, which has to be persistently exciting of a sufficiently high order.

The least-squares problem (15) is to be solved online in a recursive manner, so that an adaptive control law can be formulated. In the implementation on the test bench, the recursive least squares methodology proposed by [29] has been adopted. This involves an adaptive forgetting factor that updates the covariance matrix of the estimate of Ξ only in the direction defined by the current input–output data vector. This method gives a relatively fast estimation method with low sensitivity to noise or loss of persistency of excitation. Thus, at time k , we have $\hat{\Xi}_k$, which is the estimate of the Markov parameters at discrete time k .

$$\hat{\Xi}_k = \begin{bmatrix} \widehat{CA}^{(p-1)}\widehat{B} & \widehat{CA}^{(p-2)}\widehat{B} & \dots & \widehat{CB} & \widehat{D} & \widehat{CA}^{(p-1)}\widehat{K} & \widehat{CA}^{(p-2)}\widehat{K} & \dots & \widehat{CK} \end{bmatrix}_k. \quad (16)$$

Observe that by partitioning the matrix $\hat{\Xi}_k$ the matrices $(\tilde{\Gamma}^{(p)}\widehat{\mathcal{H}}_u^{(p)})_k$ and $(\tilde{\Gamma}^{(p)}\widehat{\mathcal{H}}_y^{(p)})_k$ can be constructed. Further, it is evident that the Toeplitz matrix estimates $\hat{H}_k^{(p)}$ and $\hat{G}_k^{(p)}$ can also be generated by the correct juxtaposition of the partitioned block matrices of $\hat{\Xi}_k$. These matrix estimates can now be used in a novel manner to formulate a repetitive control law.

3.3. Step 3: Infinite horizon repetitive control

In this subsection, the formulation of an ILC law with basis functions, as described in [30] is extended to RC. The RC law with basis functions can be stated to have the form:

$$\theta_{j+1} = \alpha \theta_j + \beta \begin{bmatrix} \delta x_j \\ \epsilon_{j-1} \end{bmatrix},$$

with

$$U_k^{(p)} = U_f \theta_j.$$

Here, j is the iteration number. One iteration in this context is defined as equal to the period P . The term $\beta \in \mathbb{R}^{b \times (n+l)}$ is the learning gain matrix, and the term α is a Q-filter (a similar ILC law can be found in [6]).

In order to reduce the dimensionality of the control input optimisation problem, the control input is taken as a linear combination of basis functions, where the subspace spanned by the basis vectors is of a lower order than the dimensionality of the control input. Thus, we have that

$$U_f = [\phi_0, \phi_1, \dots, \phi_b],$$

where each $\phi_i \in \mathbb{R}^r$ is a basis vector and $b \leq r$, and typically b is much smaller than r . The vector $\theta_k \in \mathbb{R}^b$ is an unknown vector of

coefficients that maps the control input into the basis function space. If we define $U_f = I_{r \times r}$ then the “traditional” RC controller with a full-dimensional input space is recovered. Thus, traditional RC can be considered to be a special case of RC with basis functions, for one particular basis function subspace (defined by $I_{r \times r}$).

For RC with basis functions, the change in the projected control input sequence, from one period to the next, is a function of the new initial state of the system δx_j and the reference tracking (or disturbance rejection) error ϵ_{j-1} . For traditional RC, this is equivalent to a full control input update that occurs every iteration.

The objective of this section is to define a repetitive control law that minimises the output error, or vibration output, over an infinite horizon, by manipulating the control input. The requirement of minimisation over an infinite horizon ensures asymptotic closed-loop stability for the case where the true system parameters are identified in the previous step. The predictor from Eq. (9) is hence restated here, substituting the system matrices by their estimates available at time k :

$$\delta Y_{k+p}^{(p)} = \left[(\tilde{\Gamma}^{(p)}\widehat{\mathcal{H}}_u^{(p)})_k, (\tilde{\Gamma}^{(p)}\widehat{\mathcal{H}}_y^{(p)})_k \right] \begin{bmatrix} \delta U_k^{(p)} \\ \delta Y_k^{(p)} \end{bmatrix} + \left[\hat{H}_k^{(p)}, \hat{G}_k^{(p)} \right] \begin{bmatrix} \delta U_{k+p}^{(p)} \\ \delta Y_{k+p}^{(p)} \end{bmatrix}.$$

The predicted output is at both on the righthand side and the lefthand side. This can be rewritten as:

$$\delta Y_{k+p}^{(p)} = \left[(\Gamma^{(p)}\widehat{\mathcal{H}}_u^{(p)})_k, (\Gamma^{(p)}\widehat{\mathcal{H}}_y^{(p)})_k \right] \begin{bmatrix} \delta U_k^{(p)} \\ \delta Y_k^{(p)} \end{bmatrix} + \hat{H}_k^{(p)} \delta U_{k+p}^{(p)}. \quad (17)$$

This can be proved by considering that the following equalities also hold for the estimates of the matrices:

$$\begin{aligned} (I_{p\ell} - \hat{G}_k^{(p)}) (\Gamma^{(p)}\widehat{\mathcal{H}}_u^{(p)})_k &= (\tilde{\Gamma}^{(p)}\widehat{\mathcal{H}}_u^{(p)})_k; \\ (I_{p\ell} - \hat{G}_k^{(p)}) (\Gamma^{(p)}\widehat{\mathcal{H}}_y^{(p)})_k &= (\tilde{\Gamma}^{(p)}\widehat{\mathcal{H}}_y^{(p)})_k; \\ (I_{p\ell} - \hat{G}_k^{(p)}) \hat{H}_k^{(p)} &= \hat{H}_k^{(p)}. \end{aligned}$$

Since the absolute output is to be penalised in the optimisation problem, the left hand side of the Eq. (17) is expanded:

$$Y_{k+p}^{(p)} = \left[(\Gamma^{(p)}\widehat{\mathcal{H}}_u^{(p)})_k, (\Gamma^{(p)}\widehat{\mathcal{H}}_y^{(p)})_k, I_{p\ell} \right] \begin{bmatrix} \delta U_k^{(p)} \\ \delta Y_k^{(p)} \\ Y_k^{(p)} \end{bmatrix} + \hat{H}_k^{(p)} \delta U_{k+p}^{(p)}.$$

This equation is reformulated into a state-transition form, so that an optimal state feedback matrix can be synthesised in an LQR (linear quadratic regulator) sense. Such an LQR optimal problem has been implemented in [31] for a full ILC problem without basis functions. To be emphasised is that this formulation can be done directly from online identified system parameters, and hence forms an adaptive control law. In the following LQR formulation, the vibration output over an infinite horizon is minimised [31]. Such an LQR feedback structure guarantees stability under the condition that the true system parameters are identified in the identification process:

$$\underbrace{\begin{bmatrix} Y_k^{(p)} \\ \delta U_k^{(p)} \\ \delta Y_k^{(p)} \end{bmatrix}}_{x_{j+1}} = \underbrace{\begin{bmatrix} I_{p\ell} & (\Gamma^{(p)}\widehat{\mathcal{H}}_u^{(p)})_{k-p} & (\Gamma^{(p)}\widehat{\mathcal{H}}_y^{(p)})_{k-p} \\ \mathbf{0}_{p\ell \times p\ell} & \mathbf{0}_{p\ell} & \mathbf{0}_{p\ell \times p\ell} \\ \mathbf{0}_{p\ell} & (\Gamma^{(p)}\widehat{\mathcal{H}}_u^{(p)})_{k-p} & (\Gamma^{(p)}\widehat{\mathcal{H}}_y^{(p)})_{k-p} \end{bmatrix}}_{A_j} \underbrace{\begin{bmatrix} Y_{k-p}^{(p)} \\ \delta U_{k-p}^{(p)} \\ \delta Y_{k-p}^{(p)} \end{bmatrix}}_{x_j} + \underbrace{\begin{bmatrix} \hat{H}_{k-p}^{(p)} \\ I_{p\ell} \\ \hat{H}_{k-p}^{(p)} \end{bmatrix}}_{B_j} \delta U_k^{(p)},$$

with $j \in [0, 1, 2, \dots]$ the iteration number. It is seen that the state transition and input matrices are updated at every discrete time instant k . It is known that for a wind turbine system, the dynamics change slowly over time. Hence, if the matrices are updated once every iteration, it is assumed that the approximation error is not

significant. Thus, \mathcal{A}_j and \mathcal{B}_j are taken to be functions of the iteration number j .

The input is now expressed as a linear combination of the basis functions, by the transformation $U_k^{(P)} = U_f \theta_j$, as also done in [30]. Also, the output is projected onto the subspace defined by the basis vectors, using the transformation $\bar{Y}_j = U_j^\dagger Y_k^{(P)}$, where the \dagger symbol indicates the pseudo-inverse of a matrix. The transformed state-space system is now given by

$$\begin{bmatrix} \bar{Y}_j \\ \delta \theta_j \\ \delta \bar{Y}_j \end{bmatrix}_{\bar{x}_{j+1}} = \begin{bmatrix} I_{bt} & U_j^\dagger (I^{(P)} \widehat{\mathcal{K}}_u^{(P)})_{k-p} U_f & U_j^\dagger (I^{(P)} \widehat{\mathcal{K}}_y^{(P)})_{k-p} U_f \\ \mathbf{0}_{br \times bt} & \mathbf{0}_{br} & \mathbf{0}_{br \times bt} \\ \mathbf{0}_{bt} & U_j^\dagger (I^{(P)} \widehat{\mathcal{K}}_u^{(P)})_{k-p} U_f & U_j^\dagger (I^{(P)} \widehat{\mathcal{K}}_y^{(P)})_{k-p} U_f \end{bmatrix} \begin{bmatrix} \bar{Y}_{j-1} \\ \delta \theta_{j-1} \\ \delta \bar{Y}_{j-1} \end{bmatrix}_{\bar{x}_j} + \begin{bmatrix} U_j^\dagger \widehat{H}_{k-p}^{(P)} U_f \\ I_{br} \\ U_j^\dagger \widehat{H}_{k-p}^{(P)} U_f \end{bmatrix} \delta \theta_j.$$

For synthesising an SPRC controller, the weighted norm of the quantity \bar{Y}_k over an infinite horizon is to be minimised. Thus, the cost criterion to be minimised is

$$J = \sum_{j=0}^{\infty} \|(\bar{x}_{j+1})^T Q_f \bar{x}_{j+1} + (\delta \theta_j)^T R_f \delta \theta_j\|_2^2, \quad (18)$$

where Q_f and R_f are user-defined positive-definite weighting matrices, similar to those used for a conventional LQR problem. The SPRC problem is essentially similar to the LQR problem formulation, the key difference being that SPRC involves lifting the system over one period P and projecting the input–output signals onto a basis function subspace. The state feedback gain K_f can now be obtained by solving the SPRC problem, using its similarity to the LQR formulation. A short note on the stability of the closed-loop system is given in the Section 3.3.1.

As in an ordinary LQR problem, the matrices Q_f and R_f can be tuned to increase or reduce the weighting on the control effort. Thus, a high value for Q_f and a low value for R_f indicates cheap control effort, yielding faster convergence to optimal control and vice versa. It is generally advisable to use an adequately high value for R_f from robustness considerations. For simplicity, the matrices Q_f and R_f may be chosen to be diagonal.

Now, the discrete algebraic Riccati equation (DARE) can be solved online at each time step to obtain the optimal state feedback gain K_{fj} . There are several numerically stable approaches to obtain the solution to the DARE, as given in [32]. In this manner, it is possible to synthesise a control law based directly on the Markov parameters available from the identification step, and this completes the formulation of an adaptive repetitive control law. The input sequence to be implemented for the next iteration is given by

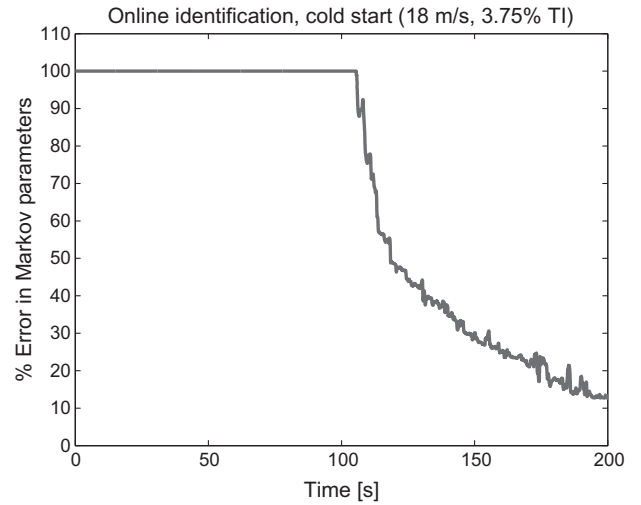


Fig. 4. The error in online identification of system Markov parameters, 18 m/s and 3.75% turbulence. [Identification starts after 100 s mark].

$$\delta U_{k+p}^{(P)} = U_f K_{fj} U_f^\dagger \begin{bmatrix} Y_k^{(P)} \\ \delta U_k^{(P)} \\ \delta Y_k^{(P)} \end{bmatrix}. \quad (19)$$

The implementation used is shown in Fig. 3. It can be seen that instead of using a fixed U_f matrix, it is synthesised online based on the azimuth angle measurement from the wind turbine. This strategy can be used directly if the basis functions are sinusoidal, and it accounts for variations in the speed of the rotor.

Since this control input contains energy only along the basis vector directions, the shape of the input signal and hence its frequency content can be controlled to a large extent. Further, the RC approach is much more robust to model uncertainty and it is hence not required to pass the controller output through a low-pass filter, but can be directly applied as a pitch actuation signal.

3.3.1. Note on stability

In case the identification process does not arrive at the true system parameters, but the true system parameters are time-invariant, then the RC controller will still be closed-loop stable as long as the deviation of the identified parameters is bounded. This bound on parametric uncertainty can be derived by extending the analysis

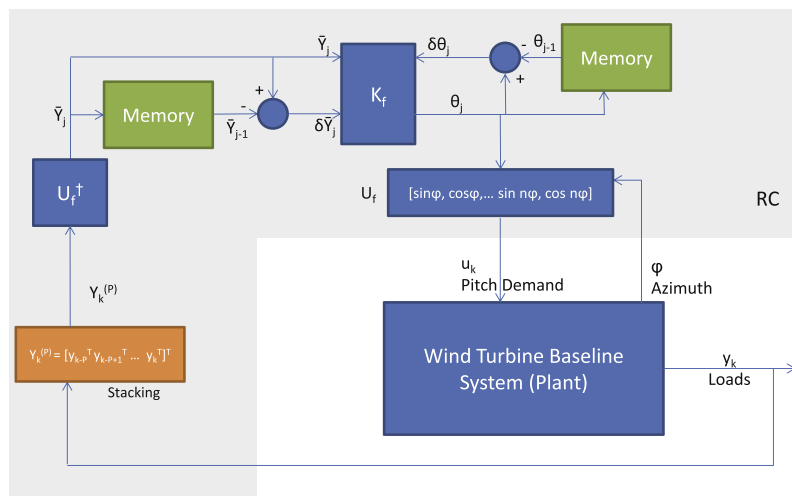


Fig. 3. RC implementation, corresponding to Eq. (19).

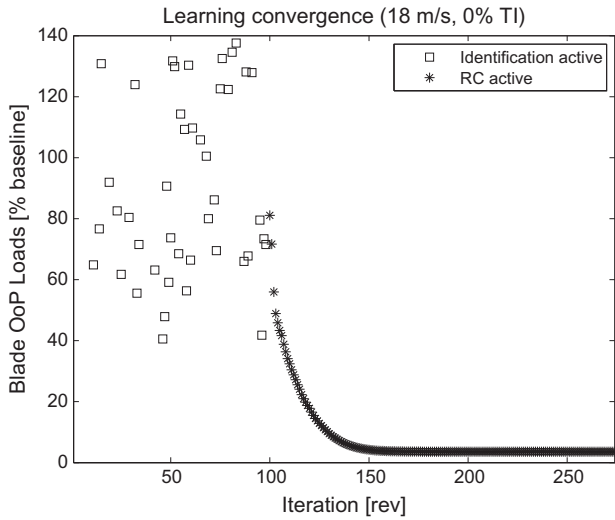


Fig. 5. Convergence of learning algorithm, 18 m/s and 0% turbulence. Identification and Repetitive Control phases not jointly active.

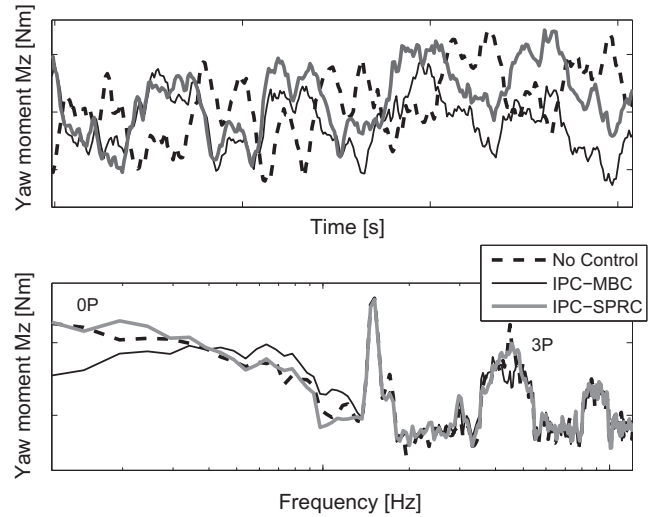


Fig. 7. Yaw bearing yawing moment, 18 m/s and 3.75% turbulence. SPRC and MBC controllers achieve reduction in mean loading and 3P frequency peak. Action of SPRC confined to dominant frequency component, MBC affects broader range of frequencies.

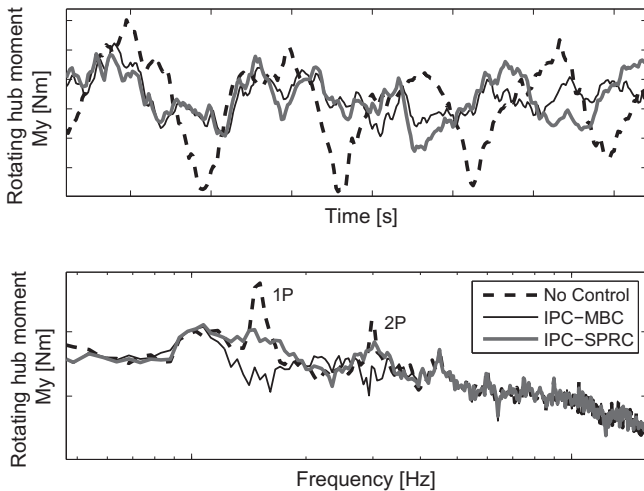


Fig. 6. Blade out-of-plane bending moment, 18 m/s and 3.75% turbulence. SPRC and MBC controllers achieve reduction in 1P and 2P frequency peaks. Action of SPRC confined to most dominant frequency components, MBC affects broader range of frequencies.

made in [33], however only the nominal case is considered in this paper. When the system parameters also vary with time, no statement can be made regarding the stability of the adaptive control law; this may still be considered to be an open problem. The assumption made for this application is that the system parameters vary slowly with time and the persistency of excitation is such that the identification reaches parameter estimates within the bounds for closed-loop stability of the system, at all instants of time.

4. Test bench implementation

The proposed SPRC controller has been tested in the simulation environment GH Bladed, as described in Section 2. The Bladed model of the XD115-5 MW was made available by XEMC Darwind BV. A baseline controller that closely follows the actual turbine controller was also available, and connected in closed-loop with this model. The SPRC controller developed as according to the formulation above was connected in feedback with this stable nominal baseline closed-loop wind turbine system.

To design a new turbine prototype, Bladed is widely used in the industry to verify that the IEC standards are met [34]. The standards specify that the turbine model should be tested in normal production mode in a representative turbulent (but stochastically stationary) wind field for periods of a duration of 600 s. The dynamic loading results of such time series are then extrapolated to determine the cumulative component fatigue damage that will occur over the turbine lifetime.

In the current case, a mean wind speed of 18 m/s is chosen for the simulations. For the wind turbine, this occurs in the above-rated region, as such, IPC is expected to be active at this wind speed. This wind speed is deemed to cause noticeably high periodic loading, and for a representative wind turbine site, will have a relatively high probability of occurrence over its lifetime.

Wind fields of four different turbulence intensities (= ratio of standard deviation of wind speed time series to the average wind speed) are simulated: 0%, 3.75%, 6% and 14%. This would be the commonly encountered range of turbulence intensities at a typical wind turbine location. 0% turbulence will not occur in practice; it has been simulated to evaluate the maximum of the load control potential achieved by this method.

For this case, it is found that most of the energy in the vibrations is concentrated at 1P and 2P (for rotating loads). Hence, the basis functions used are

$$U_f = \begin{bmatrix} \sin(2\pi/P) & \cos(2\pi/P) & \sin(4\pi/P) & \cos(4\pi/P) \\ \sin(4\pi/P) & \cos(4\pi/P) & \sin(8\pi/P) & \cos(8\pi/P) \\ \vdots & \vdots & \vdots & \vdots \\ \sin(2\pi) & \cos(2\pi) & \sin(4\pi) & \cos(4\pi) \end{bmatrix}$$

SPRC simulations have a duration of 900 s. As we expect the control strategy to converge to the optimal one from cold start, the system Markov parameters and the learning gain matrix are both initialised to 0. SPRC is then rolled out as follows,

- The first 40 cycles are run with no IPC active. This is to allow the wind turbine states of the simulation environment to settle to stationary values; and to avoid any interference of the control strategy with incorrect initial condition errors.
- For the next 60 cycles, a filtered pseudo-random binary signal with a maximum value of 3° is superposed on top of the collec-

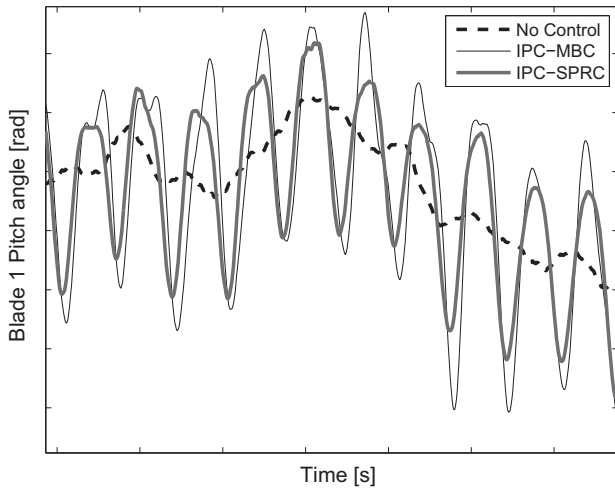


Fig. 8. Pitch angle Blade1, 18 m/s and 3.75% turbulence. Mean pitch variation of baseline followed by IPC controllers. SPRC shows phase lead and smaller amplitudes as compared to MBC.

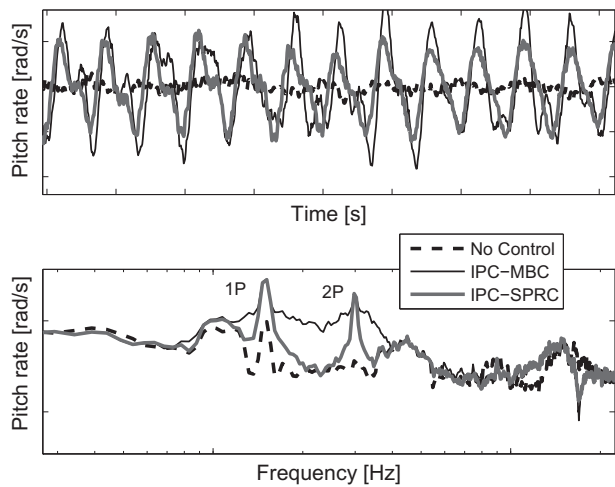


Fig. 9. Pitch angle rate Blade1, 18 m/s and 3.75% turbulence. Both IPC controllers contribute equal pitch activity at 1P and 2P. Frequency spread of MBC controller significantly larger than that for SPRC.

tive pitch demand of each blade, so as to ensure persistence of excitation. At the same time, the Markov parameters are recursively updated using the RLS methodology delineated above.

- At the end of the 60 cycles, it is assumed that adequate information on the system dynamics has been collected, and a learning gain matrix is formulated online. The parameters are updated by the learning law after each iteration; thus IPC by repetitive control is now implemented.

The identification phase starts after roughly 100 s and the strategy is able to converge to the true Markov parameters from a cold start within 100 s. Here, it is assumed that the value of past window p is 20, to increase the speed of the identification. The norm of the error between the identified Markov parameters and the true Markov parameters is shown in Fig. 4. It can be seen that the convergence is smooth and adequately rapid. The variance accounted for (vaf) at the end of the identification is more than 92%, and it seems to be reasonably high for formulating the control law.

The learning gain is calculated online from the Markov parameters, and RC is implemented. The RC is stable and converges quickly to the optimal feedforward control signal. The convergence of the learning algorithm is shown in Fig. 5, where the standard deviation of the output error during each iteration is plotted against the iteration number. It can be seen that initially, when control is not active, the error is random and denoted by the squares. Once the learning algorithm starts up, the error decays monotonically and rapidly by a factor of 17 within 50 iterations. The error in this region, i.e. when RC starts after 100 cycles, is depicted by stars. The conditions chosen for this plot are 18 m/s wind speed and 0% turbulence, to obtain a clearer picture of the behaviour of the algorithm.

The load reduction achieved by implementing this strategy has been tabulated for easy comparison. Some selected plots are also given to illustrate the region where load reduction occurs. The following load time series and spectra are compared with:

- Wind turbine simulations with only baseline controller in feedback, no IPC implemented,
- Wind turbine simulations with a conventional MBC IPC controller, for 1P and 2P frequencies, tuned for maximum hub load reduction, as per [4].
- Wind turbine simulations with SPRC IPC.

Table 2
Load reduction results.

$v_0 = 18$ m/s I_T (%)	0	3.75	6	14
% Reduction over baseline in Standard deviation of Rotor Hub Out-of-plane loads				
IPC-MBC	88.59%	51.05%	43.36%	20.99%
IPC-SPRC	93.02%	44.35%	30.52%	23.01%
% Reduction over baseline in Standard deviation of Blade Flap loads				
IPC-MBC	17.26%	15.94%	16.57%	11.96%
IPC-SPRC	17.72%	15.64%	11.08%	16.14%
% Reduction over baseline in Mean of Yawing moment				
IPC-MBC	0.60%	10.57%	24.34%	23.26%
IPC-SPRC	5.83 %	4.29%	28.77 %	14.74%
% Reduction over baseline in Mean of Tower side-side moment				
IPC-MBC	19.57%	19.67%	19.59%	19.19%
IPC-SPRC	19.06%	19.44%	19.91%	22.37%
Standard deviation of Pitch Angle Rates (°/s)				
IPC-MBC	1.354	1.51	1.76	2.334
IPC-SPRC	1.331	1.378	1.432	1.467

Fig. 6 depicts the reduction in the out-of-plane bending load on the blade root and the hub, one of the key design variables. It can be seen that the dominant peaks at 1P and 2P are damped well by both controllers. The MBC controller affects more frequencies than the SPRC controller, which selectively targets only 1P and 2P. Fig. 7 shows the reduction in the yawing moment on the yaw bearing caused by IPC. The yaw bearing, like all structural components in the stationary frame, shows dominant loading at 3P, which is reduced by both controllers. The mean of the yaw load is also reduced by IPC. The peak at 1P is caused by mass or aerodynamic imbalance and is not addressed by IPC in the current form.

Fig. 8 shows the variation of the pitch angle of one of the blades over time. It can be seen that the pitch angle for the collective pitch varies much more slowly, while the IPC controllers superpose a periodic variation on top of this. SPRC control commands are lower than those of MBC-IPC, and it is also interesting to note that the SPRC controller, as a quasi-feedforward controller, shows phase lead over the control action of the feedback IPC controller. In Fig. 9, the advantage of SPRC can be seen since the pitch rate demand is lower, and the frequency is strictly controlled to the two allowed frequencies of 1P and 2P. On the other hand, the IPC-MBC pitch rate demand contains a much broader spectrum of frequencies (see Table 2).

The same trend is found for other values of turbulence intensity, as given in the table. Similar levels of load reduction are observed in almost all cases for the two IPC controllers. However, while the pitch activity is almost the same for 0% turbulence, it rises much more modestly with turbulence for SPRC than for MBC.

5. Conclusions

Active load reduction for wind turbines by modifying the aerodynamic flow around each blade individually poses a challenge to the control engineer on account of the highly coupled MIMO structure. As seen from the literature, the MBC transform is used to decouple the system to facilitate tuning of a new controller for each frequency to be addressed. However, as the results in this paper, as well as recent literature show, there is very little control on the actuator signals, which have severe practical constraints. Also, each turbine needs to be tuned independently since its dynamics are not known prior to installation, and change during operation.

In this paper, we devise a novel methodology, Subspace Predictive Repetitive Control, which combines online data-driven black box system identification with basis function learning control to overcome the issues of unknown dynamics and control over input frequency content. A data-driven RLS technique is adopted to identify the Markov parameters of the system from the differenced input–output data. The repetitive control law is devised optimally for an infinite horizon in an LQR sense, using input and output data as the state of the extended system.

SPRC is implemented on an industrial wind turbine simulation environment and it shows relatively rapid and stable learning. In the optimal case, it can entirely eliminate the periodic disturbances in the directions of the basis function vectors. The SPRC methodology is also able to deal with the more realistic case of turbulent wind fields, and shows performance equivalent to that of a conventional IPC controller, with much smoother control input, and reduced input energy.

Thus, starting from zero a priori knowledge of the system, SPRC is able to learn the dynamics of the wind turbine as well as the optimal feedforward control sequence for disturbance suppression, and achieves the same performance as a state-of-the-art reference controller; at the same time enforcing a superior control input behaviour.

Acknowledgments

This work was supported by XEMC-Darwind BV, which owns the prototype wind turbine under purview.

References

- [1] Gsänger S, Pitteloud J-D. *World wide energy report 2012*. World Wind Energy Association 2012.
- [2] Nijssen RPL. *Fatigue life prediction and strength degradation of wind turbine rotor blade composites*. PhD thesis, Delft University of Technology; 2006.
- [3] Steinbuch M. *Dynamic modelling and robust control of a wind energy conversion system*. PhD thesis, Delft University of Technology; 1989.
- [4] Bossanyi EA. *Individual blade pitch control for load reduction*. *Wind Energy* 2003;6(2):119–28.
- [5] Arimoto S, Kawamura S, Miyazaki F. *Bettering operation of robots by learning*. *J Robotic Syst* 1984;1:123–40.
- [6] Bristow DA, Tharayil M, Alleyne AG. *A survey of iterative learning control*. *IEEE Contr Syst Mag* 2006;96–114.
- [7] Tousain R, van Casteren D. *Iterative learning control in a mass product: light on demand in DLP projection systems*. In: *Proceedings of the American control conference*, New York City, USA; 2007.
- [8] van de Wijdeven J, Bosgra OH. *Hankel iterative learning control for residual vibration suppression with mimo flexible structure experiments*. In: *Proceedings of the American control conference*, New York City, USA; 2007.
- [9] Wang L, Gawthrop P, Owens DH, Rogers E. *Switched linear predictive controllers for periodic exogenous signals*. *Int J Contr* 2010;83:848–61.
- [10] Houtzager I, van Wingerden JW, Verhaegen M. *Wind turbine load reduction by rejecting the periodic load disturbances*. *Wind Energy* 2013;16:235–56.
- [11] van de Wijdeven J, Bosgra OH. *Using basis functions in iterative learning control: analysis and design theory*. *Int J Contr* 2010;83:661–75.
- [12] Bolder J, Oomen T, Steinbuch M. *Exploiting rational basis functions in iterative learning control*. In: *Proceedings of the 51st IEEE conference on decision and control*, Florence, Italy; 2013.
- [13] van Wingerden JW, Hulskamp A, Barlas T, Houtzager I, Bersee HEN, van Kuik GAM, et al. *Two-degree-of-freedom active vibration control of a prototyped smart rotor*. *IEEE Trans Contr Syst Technol* 2010;284–96.
- [14] Frueh JA, Phan MQ. *Linear quadratic optimal learning control (LQL)*. *Int J Contr* 2000;10:832–9.
- [15] Ye Y, Wang D. *DCT basis function learning control*. *IEEE/ASME Trans Mechatr* 2005;10:449–54.
- [16] Verhaegen M, Verdult V. *Filtering and system identification: an introduction*. Cambridge University Press; 2007.
- [17] Favoreel W, de Moor B, van Overschee P, Gevers M. *SPC: subspace predictive control*. In: *Proceedings of the IFAC World Congress*, Beijing; 1998.
- [18] van der Veen GJ. *Identification of wind energy systems*. PhD thesis, Delft University of Technology; 2013.
- [19] Manwell JF, McGowan JG, Rogers AL. *Wind energy explained: theory, design and application*. Chichester: John Wiley and Sons Ltd; 2002.
- [20] XEMC-Darwind BV. website XEMC-Darwind, www.xemc-darwind.com, 2013. Last visited 02 September; 2013.
- [21] Bossanyi EA. *The design of closed loop controllers for wind turbines*. *Wind Energy* 2000;3:149–63.
- [22] Laks JH, Pao LY, Wright AD. *Control of wind turbines: past, present and future*. In: *Proceedings of the American control conference*, St. Louis, Missouri, USA; 2009.
- [23] Bossanyi EA. *Further load reductions with individual pitch control*. *Wind Energy* 2005;8:481–5.
- [24] Bottasso CL, Croce A, Riboldi CED, Nam Y. *Multi-layer control architecture for the reduction of deterministic and non-deterministic loads on wind turbines*. *Renew Energy* 2013;51:159–69.
- [25] Stol KA, Zhao W, Wright AD. *Individual blade pitch control for the controls advanced research turbine CART*. *J Solar Energy Eng* 2006;128:498–505.
- [26] van Engelen TG. *Design model and load reduction assessment for multi-rotational mode individual pitch control (higher harmonics control)*. In: *Proceedings of the European wind energy conference*, Athens, Greece; 2006.
- [27] Lackner AL, van Kuik GAM. *A comparison of wind turbine smart rotor control approaches using trailing edge flaps and individual pitch control*. *Wind Energy* 2010;13:117–34.
- [28] Chiuso A. *The role of vector auto regressive modeling in predictor based subspace identification*. *Automatica* 2007;43(6):1034–48.
- [29] Kulhavy R. *Restricted exponential forgetting in real-time identification*. *Automatica* 1987;23:589–600.
- [30] van de Wijdeven J, Bosgra OH. *Using basis functions in iterative learning control: analysis and design theory*. *Int J Contr* 2010;83:661–75.
- [31] Dijkstra BG, Bosgra OH. *Extrapolation of optimal lifted system ILC solution, with application to a waferstage*. In: *Proceedings of the American control conference*, Anchorage, Alaska, USA; 2002.
- [32] Arnold III WF, Laub AJ. *Generalised eigenproblem algorithms and software for algebraic Riccati equations*. *Proc IEEE* 1984;72:1746–54.
- [33] Martin JM. *State-space measures for stability robustness*. *IEEE Trans Automatic Contr* 1987;AC-32(6):509–12.
- [34] International Electrotechnical Commission. IEC 61400-1, wind turbines - part 1: design requirements. Geneva, Switzerland; 2005.